Kinesin expands and stabilises the GDP-microtubule lattice

Daniel R. Peet, Nigel J. Burroughs & Robert A. Cross

Supplementary Information

- Supplementary Figures 1-5
- Supplementary Tables 1-2
- Supplementary Methods
- Legends to Supplementary Videos 1-5
- Legend to Supplementary Animation 1

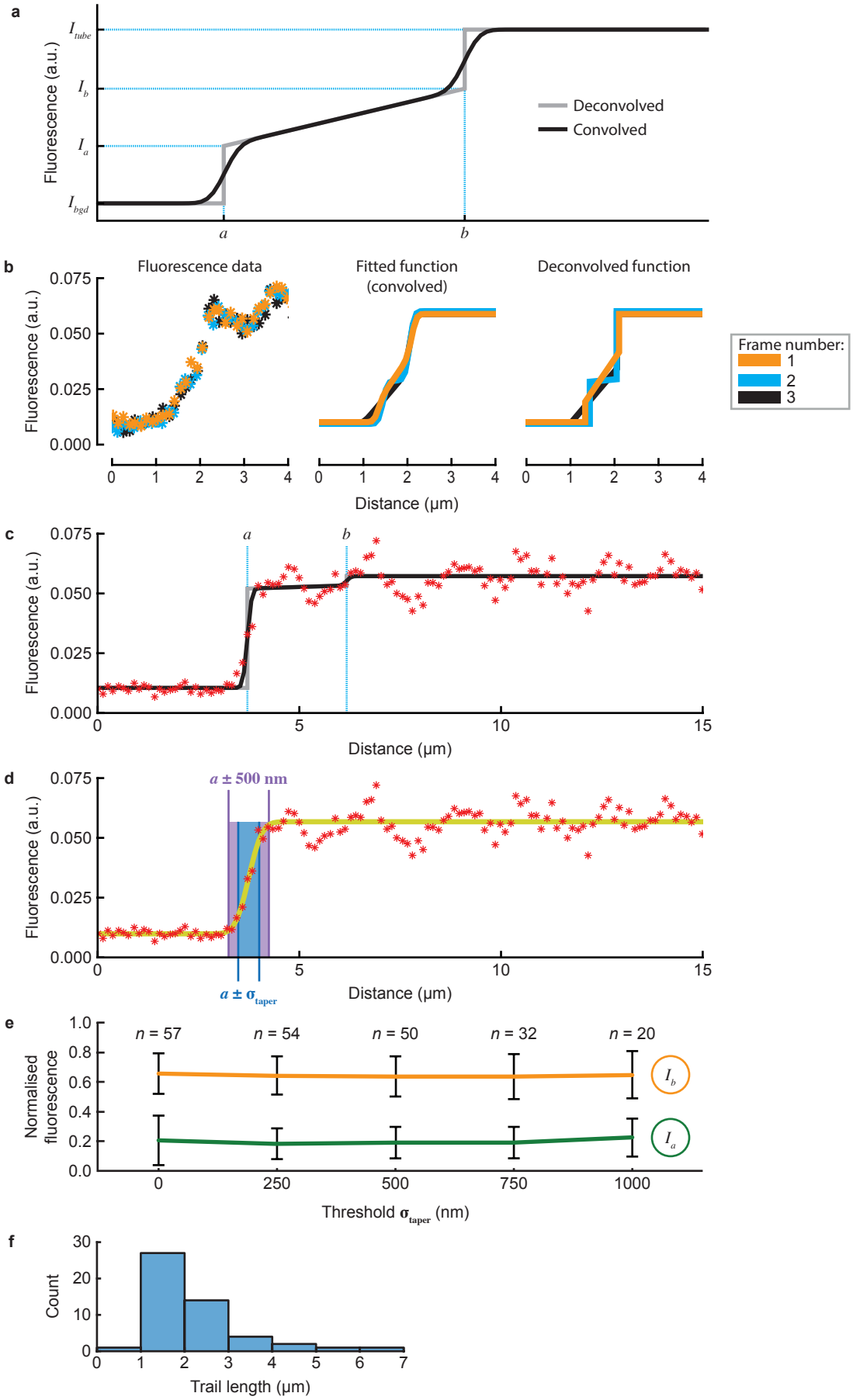

Supplementary Figure 1 | Quantifying MT fluorescence profiles with a stepped tip function. a, Schematic of the stepped tip function before and after convolution with the point-spread function of the microscope (Gaussian approximation). Points *a* and *b* mark the tip and base of the trail, where I_a and I_b are the respective fluorescence intensities. I_{bgd} is the background signal and I_{tube} is that of the MT. **b,** Time-lapse intensity profile of a blunt-ended MT in a nucleotide-free kinesin-clamp (4 second time interval). Parameter values are sensitive to small fluctuations when trails are short. **c,** Erroneous trail detection at a blunt MT tip. If the MT is blunt-ended, a trail is accommodated within the noise of the MT signal and predicted trail lengths are sensitive to small intensity fluctuations. **d,** Thresholding using a 'counter-fit'. If the spread of a MT tip (σ_{taper}), which is obtained by fitting a single-step tip function (Supplementary Methods), is less than 500 nm then we classify a MT as blunt-ended and do not fit a trail, thus achieving a robust fit and avoiding the issues highlighted in **b** and **c**. **e,** Trail intensities estimates (I_a and I_b) plotted against the threshold set for σ_{taper}. The parameters are not sensitive to the threshold value. Error bars show mean ± standard deviation. **f,** Length distribution of trails used for for the quantification of trail fluorescence. The absence of trails < 1 μm in length is due to the thresholding criteria described.

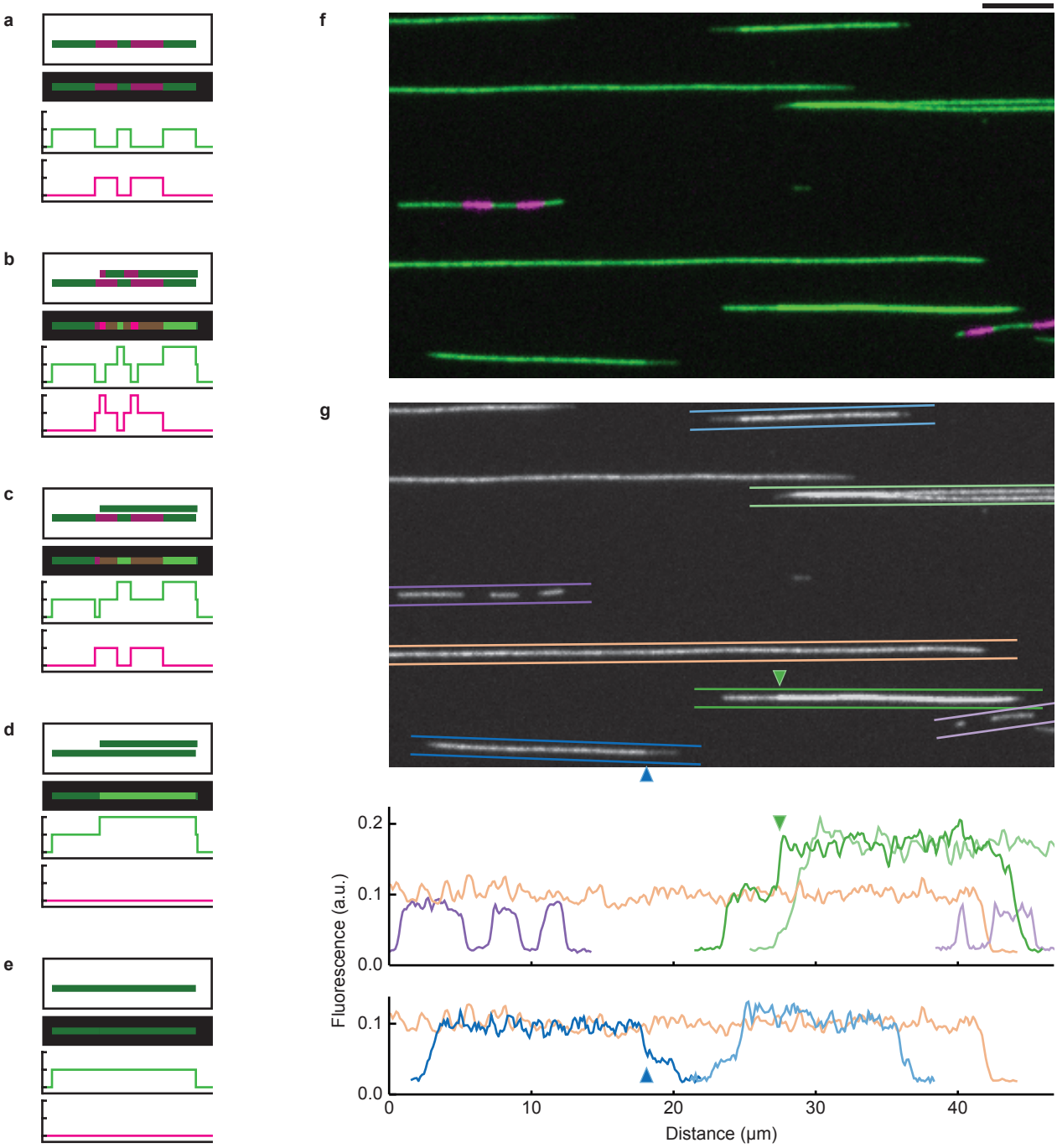

Supplementary Figure 2 | Fluorescence controls allow unambiguous identification of single MTs and MT bundles. a-e, Progressing from the top down, subpanels show schematics of (1) the number of MTs; (2) the appearance when MTs are overlaid; (3) the corresponding signal in the green channel; (4) the signal in the magenta channel. **a,** A fluorescence control, consisting of a GMPCPP-stabilised MT with a binary labelling pattern (alternating magenta and green segments). **b-c,** Fluorescence controls that are overlapping with each other or with dynamic MTs (which are shown exclusively in green) are easily identified by their intensity profiles. **d-e,** MT bundles and single MTs are distinguished by comparing the fluorescence intensity of dynamic MTs with controls (**a**). **f,** Dual-colour fluorescence image of a kinesin-clamp assay. Scale bar: 5 μm. **g,** Green channel from the image in **f** (*top*) and colour-coded vertical projections of fluorescence intensity profiles (*bottom*). Colour-coding is as follows: purple - fluorescence controls; peach - dynamic MT with no trail; green - MT bundles; blue - individual MTs with trails. Lines overlaying the image depict the cross-sectional regions used to generate the intensity profiles. Triangles highlight where bundles and individual MTs with trails might be confused if controls were not implemented.

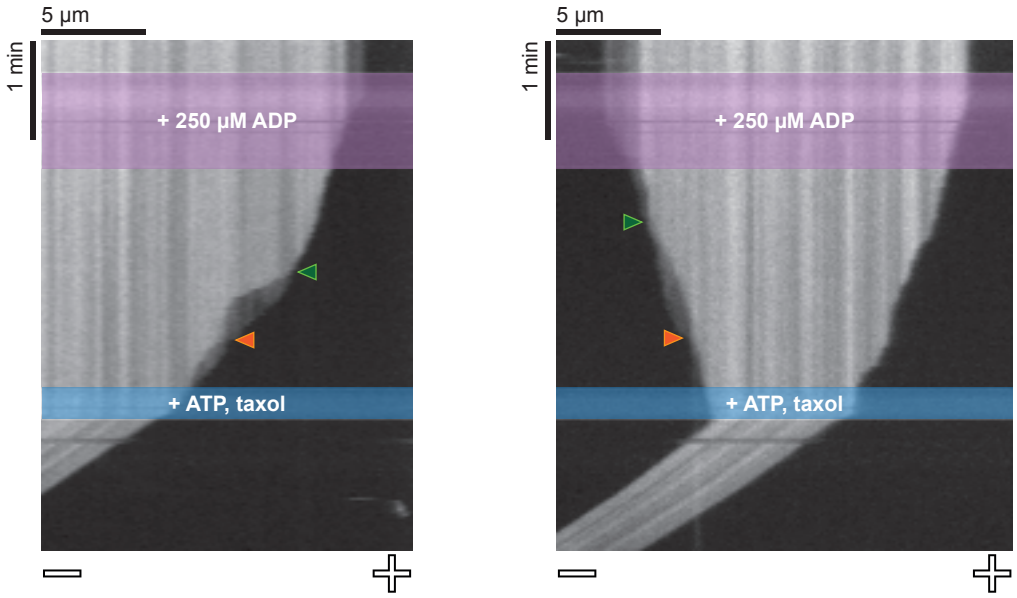

Supplementary Figure 3 | Trails commonly form, lengthen and retract at shrinking MT tips. A plus-end trail is shown in the kymograph on the left and a minus-end trail in the one on the right. In each case the green arrowhead marks where the MT begins to shrink faster than the trail, causing the trail to lengthen. The orange arrowhead marks the time when the trail rejoins the MT.

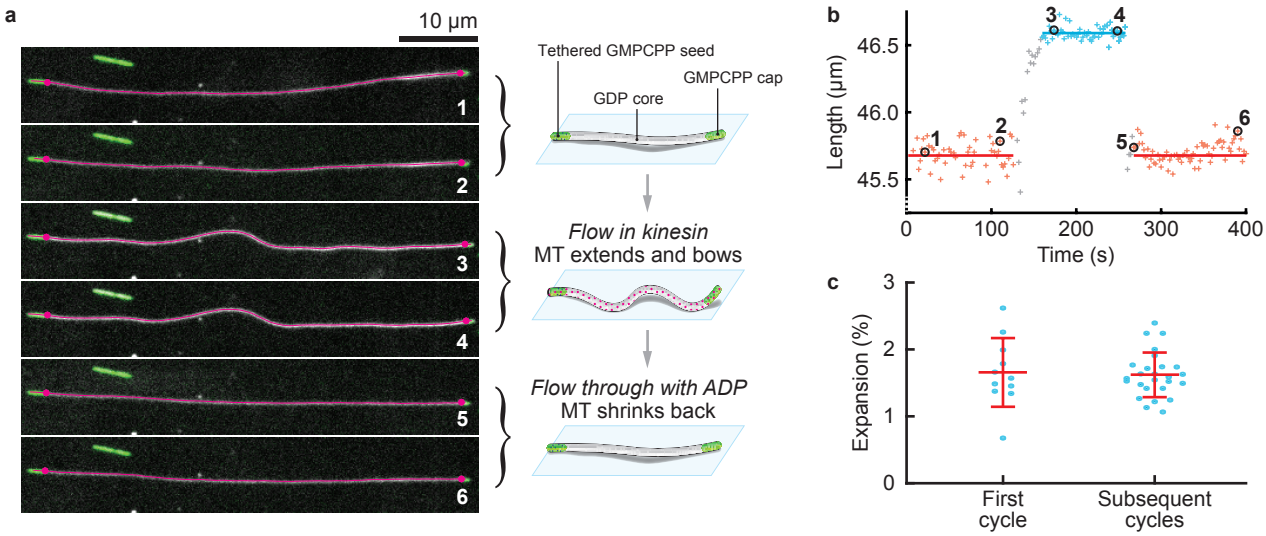

Supplementary Figure 4 | Kinesin-driven MT expansion is not significantly affected by surface stitching. a, GDP-MTs (white) were grown from stabilised, green-fluorescent GMPCPP-tubulin seeds and then also capped with GMPCPP-tubulin. Seeds were tightly bound to the surface via biotin-streptavidin linkages, whereas the rest of the MT was largely free to move (1,2). Flowing kinesin into the channel caused the MT to expand and additionally bow due to being pinned sparsely to the surface (3,4). Flushing with ADP-containing buffer encouraged detachment of kinesin from the MT and also washed out kinesin molecules in solution. The MT then quickly reverted to its original length (5,6). Further detail can be seen in Supplementary Movie 5, which also shows a second expansion-contraction cycle. The MT contour is highlighted in magenta, where circles mark the endpoints used to measure the length of the GDP-MT. **b,** Length change of the GDP-part of the MT during a kinesin-induced extend-recoil cycle. Measurements are taken from the MT as shown in a and numbering corresponds to the frames shown. Horizontal lines show the mean lengths during each phase. **c,** Relative expansion of GDP-MTs upon binding kinesin, categorised by the number of expansion-contraction cycles undertaken. Each point represents a different MT (no individual MT appears in each category). Mean ± SD (*n*) is 1.66 ± 0.51 (11) for the first cycle and 1.62 ± 0.33 (26) for subsequent cycles. Mean values are not significantly different (p = 0.80, two-tailed t-test).

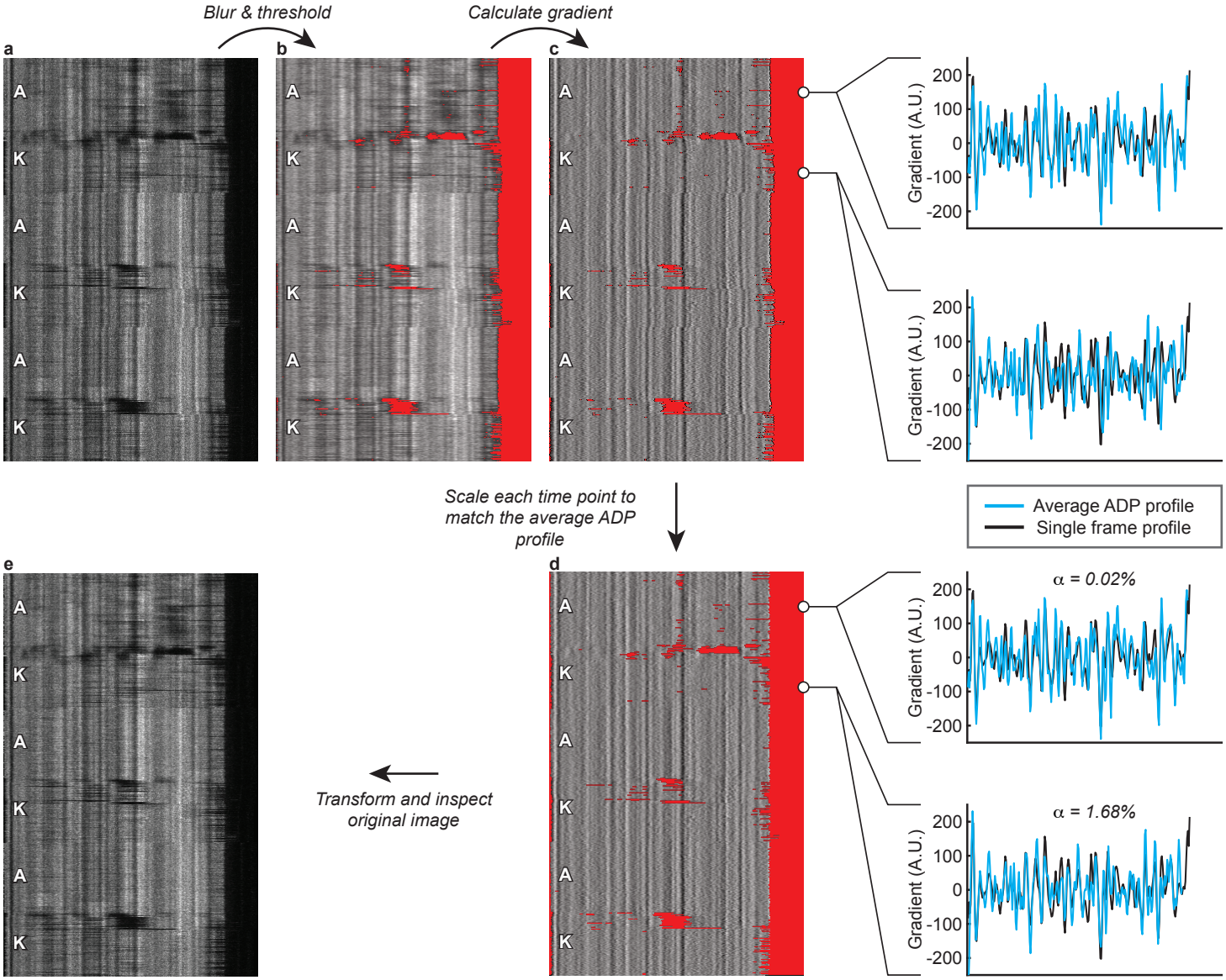

Supplementary Figure 5 | Workflow of kymograph analysis for GDP-MT expansion. a, The example shown is the kymograph from Figure 5 (magenta imaging channel). **b,** First, the kymograph was smoothed with a 1x30 gaussian kernel (σ = 1 pixel) and then thresholded to remove the background and pixels where the MT dipped out of the TIRF illumination. **c,** Next, the gradient was estimated by central difference [$y \rightarrow (y_{n+1} - y_{n-1})/2$] for each row/time point. Two graphs compare the average ADP profile (blue) to the profile of a single time point. The upper graph shows an ADP time point, which unsurprisingly matches well to the average ADP profile, whereas the lower graph shows a kinesin time point, whose peaks do not coincide with the average ADP profile. **d,** Next, we scaled each profile to match the average ADP profile, mapping $x \rightarrow x/\alpha + \beta$ and minimising the mean of square residuals while varying α and β. The varible α reflects the MT expansion measured, whereas β provides the necessary offset to align the data once it has been scaled. In the example graphs shown, only a slight scaling (α = 0.02%) improves the alignment of the upper (ADP) time point. However, the profile in the lower (kinesin) time point aligns optimally with the average ADP profile when α = 1.68%. Finally, the original kymograph was transformed as in panel **d**, and inspected to check that the analysis had performed correctly. Supplementary Animation 1 shows this transformation more clearly and in 2-colours.

Supplementary Table 1 | Shrinkage rates of MTs in a kinesin-clamp. Values shown are mean ± SEM (*n*) and correspond to the data plotted in Fig. 2d.

ADP concentration (μM)	**Shrinkage rate (dimer PF^{-1} s^{-1})**			
	Plus-end		Minus-end	
	Microtubule	Trail	Microtubule	Trail
0.4	0.06 ± 0.01 (6)	0.42 (1)	0.07 ± 0.02 (6)	0.40 ± 0.24 (4)
2	0.24 ± 0.03 (15)	1.62 (1)	0.24 ± 0.03 (13)	0.69 ± 0.14 (6)
10	1.57 ± 0.46 (10)	3.26 ± 0.44 (2)	1.40 ± 0.12 (11)	1.16 ± 0.30 (10)
50	5.08 ± 0.38 (22)	8.28 ± 0.69 (4)	3.39 ± 0.23 (20)	5.04 ± 0.68 (17)
250	3.56 ± 0.35 (18)	8.58 ± 1.25 (2)	3.22 ± 0.44 (3)	4.07 ± 0.70 (11)
1250	8.40 ± 1.87 (8)	8.42 (1)	3.74 ± 0.26 (12)	3.69 ± 0.53 (4)

Supplementary Table 2 | MT expansion under constant hydrodynamic flow. Values shown are mean ± standard deviation of the measurements and correspond to the data plotted in Fig. 5f.

	Phase		*n*		
[Kinesin] (nM)	ADP	Kinesin	Measurements	Independent experiments	MTs
25	0.00 ± 0.07	1.14 ± 0.38	11	2	5
50	0.00 ± 0.03	1.26 ± 0.18	9	1	3
100	0.03 ± 0.12	1.24 ± 0.20	5	2	3
200	0.00 ± 0.04	1.58 ± 0.18	44	5	16

Supplementary methods

1 Flat-field correction

Flat-field correction was applied to each image to ensure that fluorescence intensities were spatially unbiased. We imaged Alexa Fluor 488 dye in K-PEM over several concentrations and plotted fluorescence versus concentration for each pixel. We calculated the slope, which we confirmed to be linear in the range of concentrations used, by least squares fitting. These values were used to normalise the fluorescence intensity of kinesin-clamp images after subtracting a background (K-PEM only) image.

2 Image registration

Some stage-drift occurred during the kinesin-clamp experiments, particularly for the low [ADP] data, which naturally took longer to acquire. We corrected for this using a rigid image registration algorithm[1]. The stabilised X-rhodamine microtubule segments (from the fluorescence controls) were used to register both channels. Registrations used the starting frame in a stack as the reference image.

3 Quantification of trail intensities

The stepped tip function for approximating the fluorescence profile of microtubules with trails was defined as follows

$$\Upsilon(x) = \begin{cases} I_{bgd} & \text{if} \quad x < a \\ \dfrac{(x-a)(I_b - I_a) + I_a(b-a)}{b-a} & \text{if} \quad a \le x < b \\ I_{tube} & \text{if} \quad x \ge b, \end{cases} \tag{1}$$

where $a \le b$, $I_a \le I_b \le I_{tube}$ and I_a and I_b denote the intensity of fluorescence at points a and b, respectively (Supplementary Fig. 3a).

We generated a theoretical point-spread function (PSF) for our imaging conditions (fluorophore - Alexa Fluor 488; objective – 100x NA 1.3, 1.25x additional magnification), averaged its cross-section to mimic the procedure used for generating our kymographs and approximated it with a Gaussian curve f with standard deviation σ_{PSF}.

We normalised this PSF ($\int f = 1$) before convolving it with the stepped tip function, leading to the analytical expression

$$\begin{aligned}[\Upsilon * f](x) = \; & I_{bgd} + p[f(x-a) - f(x-b)] \\ & + q(F(x-a) - F(x-b)] + \big(I_{tube} - I_{bgd}\big)F(x-b), \end{aligned} \tag{2}$$

where

$$p = \frac{(I_b - I_a)\sigma_{\mathrm{PSF}}{}^2}{b - a}, \tag{3}$$

$$q = \frac{(I_b - I_a)(x - a) + (I_a - I_{bgd})(b - a)}{b - a} \tag{4}$$

and F is the integral of f, given by

$$F(x) = 0.5\left(1 + \mathrm{erf}\left(\frac{x}{\sigma_{\mathrm{PSF}}\sqrt{2}}\right)\right). \tag{5}$$

We then fit this convolved tip function to microtubule fluorescence intensity profiles by least squares.

4 Robust fitting

The parameters of the stepped tip function are only meaningful when a trail is present. When microtubules have short trails or no trail at all, parameter estimates are sensitive to small fluctuations in the signal (Supplementary Fig. 3b). Similarly, at blunt microtubule tips $I_a = I_b = I_{tube}$, reducing the equation above to

$$[\Upsilon * f](x) = I_{bgd} + \big(I_{tube} - I_{bgd}\big)F(x - a). \tag{6}$$

This has fewer parameters than the stepped tip function, meaning that trail length $(b - a)$ is ill defined at blunt microtubule tips. Blunt-ended microtubules are thus liable to over fitting to noise (Supplementary Fig. 3c).

Relaxing σ_{PSF} to a free parameter σ_{taper} provides a measure of how tapered microtubule tips are[2]:

$$G(x) = I_{bgd} + 0.5\big(I_{tube} - I_{bgd}\big)\left(1 + \mathrm{erf}\left(\frac{x - a}{\sigma_{\mathrm{taper}}\sqrt{2}}\right)\right). \tag{7}$$

We used this function as a 'counter fit' to ensure robust fitting of the stepped tip function; if $\sigma_{\mathrm{taper}} < 500$ nm, we classified the tip as blunt and trail parameters were not extracted (Supplementary Fig. 3d). For microtubules with $\sigma_{\mathrm{taper}} \geq 500$ nm the stepped tip function was used (Supplementary Equation 2). Results were in fact insensitive to the value of σ_{taper}, (Supplementary Fig. 3e).

5 Normalisation to fluorescence controls

The intensity profile for each segment of the fluorescence controls (2-colour barcoded stabilised microtubules) were approximated using the function

$$H(x) = I_{bgd} + 0.5\big(I_{tube} - I_{bgd}\big)\left(\mathrm{erf}\left(\frac{x - a_1}{\sigma_1\sqrt{2}}\right) - \mathrm{erf}\left(\frac{x - a_2}{\sigma_2\sqrt{2}}\right)\right), \tag{8}$$

which is analogous to function G but encompasses both ends of the microtubule, where a_1 and a_2 are the coordinates of the microtubule tips and σ_1 and σ_2 are the respective standard deviations (Supplementary Fig. 4b). Microtubule intensity is

given by $I_* = I_{tube} - I_{bgd}$ for each of the three functions. Comparing the intensity of dynamic microtubules with fluorescence controls established that only individual microtubules (and not microtubule bundles) were quantified (Supplementary Fig. 1, 4c). The reason why dynamic microtubules were slightly more intense than fluorescence controls is unclear. We suspect that Alexa Fluor 488 labelled tubulin incorporates more efficiently into GTP-microtubules than GMPCPP-microtubules.

References

1. Guizar-Sicairos, M., Thurman, S. T. & Fienup, J. R. Efficient subpixel image registration algorithms. *Opt Lett* **33,** 156–158 (2008).
2. Demchouk, A. O., Gardner, M. K. & Odde, D. J. Microtubule Tip Tracking and Tip Structures at the Nanometer Scale Using Digital Fluorescence Microscopy. *Cel. Mol. Bioeng.* **4,** 192–204 (2011).

Legends to Supplementary Movies

Supplementary Movie 1 | A kinesin-clamp assay. The image data (*top*) corresponds to the kymograph in Fig. 2c (*bottom*). A minus-end trail is clearly seen in the no nucleotide phase. Addition of ADP causes the microtubule tips to shrink. In this case, the minus-end trail is retained during shrinkage. Microtubules are re-stabilised upon addition of taxol and ATP, and the resulting kinesin-driven microtubule gliding reveals the microtubule polarity.

Supplementary Movie 2 | Strong-binding state kinesin can lock the curvature of GDP-microtubules. For each concentration of T93N, images are sorted according to the microtubule orientation. The marked microtubules in each row (*orange asterisks*) fall into the orientation range depicted by the protractor diagrams (*left*). Microtubules are straight and dynamically unstable at the beginning of the movie. Arrows (*top*) highlight the presence and direction of hydrodynamic flow, which causes microtubule bending. In the absence of kinesin, stopping the flow causes the microtubules to re-straighten and continue to depolymerise. Microtubule curvature is preserved at low concentrations of T93N but not at high concentrations. Microtubules also transiently crinkle when T93N is flowed through at high concentrations.

Supplementary Movie 3 | Kinesin reversibly expands microtubules under constant hydrodynamic flow. The movie corresponds to the microtubule shown in Fig. 5b. As kinesin and ADP are alternately introduced into the flow, the microtubule visibly expands and contracts, most obviously seen by the downstream microtubule tip visibly shifting right and left. Both surface-free and transient surface-snagging behaviour can be seen in this movie, and the microtubule expands to the same extent in each case (Fig. 5d).

Supplementary Movie 4 | Microtubules briefly crinkle when kinesin is introduced to the flow. An ADP-to-kinesin transition is shown, during which the microtubule crinkles and thereby dips in and out of the TIRF illumination. Most of the microtubules are visibly free from the surface for the duration.

Supplementary Movie 5 | Kinesin increases the lattice spacing of surface-stitched GDP-microtubules. The movie corresponds to the microtubule shown in Fig. 5f. Part way through the movie, 200 nM of monomeric kinesin (K340) was flowed through the channel and the microtubule extends and bows so as to follow a longer path length. Flushing with 1 mM ADP triggers kinesin unbinding, and the microtubule reverts to its original length. After washing the sample thoroughly with buffer, the process can be repeated. After the first cycle, the microtubule becomes tethered to the surface at a greater number of interaction sites. During the second kinesin flow-through, part of the microtubule briefly goes out of focus but it is recruited back into the optical plane, demonstrating that our protocol restricts motion in the *z*-axis to permit reliable quantification. Arrows indicate when the solution is flowing. Scale bar is 10 μm.

Supplementary Animation 1 | Kymograph profile matching for measuring microtubule expansion. The 'original' kymograph shown is the same as in Fig. 5b. The 'transformed' kymograph is the same image but each row has been compressed by the values shown in Fig. 5d. This highlights the uniform expansion of the microtubule that occurs when kinesin binds.